AD-A094 388 AERONAUTICAL RESEARCH LABS MELBOURNE (AUSTRALIA) F/G 11/6
ACOUSTIC EMISSION FROM THE ALUMINIUM ALLOY 7050.(U)
OCT 79 S M COUSLAND, C M SCALA
UNCLASSIFIED ARL/MAT-113 NL

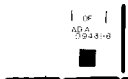

END
DATE FILMED
2-81
DTIC

ARL-MAT-REPORT-113

AR-001-779

AD A094388

DEPARTMENT OF DEFENCE

DEFENCE SCIENCE AND TECHNOLOGY ORGANISATION

AERONAUTICAL RESEARCH LABORATORIES

MELBOURNE, VICTORIA

MATERIALS REPORT 113

ACOUSTIC EMISSION FROM THE ALUMINIUM ALLOY 7050

THE UNITED STATES NATIONAL TECHNICAL INFORMATION SERVICE IS AUTHORISED TO REPRODUCE AND SELL THIS REPORT

by

S. McK. COUSLAND and C. M. SCALA

DMC FILE COPY

Approved for Public Release.

© COMMONWEALTH OF AUSTRALIA 1979

COPY No 9

OCTOBER 1979

81 2 2 082

THE UNITED STATES NATIONAL
TECHNICAL INFORMATION SERVICE
IS AUTHORISED TO
REPRODUCE AND SELL THIS REPORT

AR-001-779

DEPARTMENT OF DEFENCE
DEFENCE SCIENCE AND TECHNOLOGY ORGANISATION
AERONAUTICAL RESEARCH LABORATORIES

9) MATERIALS REPORT 113

17 AR-MAT-113

(4) ACOUSTIC EMISSION FROM THE ALUMINIUM ALLOY 7050.

11) Oct 79

by

10 S. McK. COUSLAND and C. M. SCALA

SUMMARY

Studies of the acoustic emission detected during deformation of the commercial aluminium alloy 7050 are described. Tests have been performed on unflawed tensile specimens and notched specimens of the alloy in a variety of heat-treated conditions. Attempts are made to correlate the detected emission with various microstructural features affecting the deformation of the alloy.

POSTAL ADDRESS: Chief Superintendent, Aeronautical Research Laboratories,
Box 4331, P.O., Melbourne, Victoria, 3001, Australia.

DARLCA-M

DOCUMENT CONTROL DATA SHEET

Security classification of this page: Unclassified

1. Document Numbers
   (a) AR Number:
   AR-001-779
   (b) Document Series and Number:
   Materials Report 113
   (c) Report Number:
   ARL-Mat-Report-113

2. Security Classification
   (a) Complete document:
   Unclassified
   (b) Title in isolation:
   Unclassified
   (c) Summary in isolation:
   Unclassified

3. Title: ACOUSTIC EMISSION FROM THE ALUMINIUM ALLOY 7050

4. Personal Author(s):
   Cousland, S. McK.
   Scala, C. M.

5. Document Date:
   October, 1979

6. Type of Report and Period Covered:

7. Corporate Author(s):
   Aeronautical Research Laboratories

8. Reference Numbers
   (a) Task:
   AIR 72/09, DST 76/92, DST 76/95
   (b) Sponsoring Agency:

9. Cost Code:
   326720, 344780, 344790

10. Imprint:
    Aeronautical Research Laboratories,
    Melbourne

11. Computer Program(s)
    (Title(s) and language(s)):

12. Release Limitations (of the document):
    Approved for public release

12-0. Overseas:	N.O.		P.R.	1	A		B		C		D		E	

13. Announcement Limitations (of the information on this page):
    No Limitations

14. Descriptors:

Aluminium alloys	Acoustic emission	
Deformation	Acoustic sources	
Heat treatment	Slip-band formation	
Microstructure	Failure	

15. Cosati Codes:
    2001

16. *ABSTRACT*

Studies of the acoustic emission detected during deformation of the commercial aluminium alloy 7050 are described. Tests have been performed on unflawed tensile specimens and notched specimens of the alloy in a variety of heat-treated conditions. Attempts are made to correlate the detected emission with various microstructural features affecting the deformation of the alloy.

CONTENTS

1. INTRODUCTION

Acoustic emission (AE) is being increasingly used to locate and characterize flaws in structural components during proof-testing and in actual service. Understanding of the generation, propagation, and detection of elastic waves is needed in order to interpret AE measurements and to increase our capability of using AE for flaw evaluation. The effort directed towards calibration of AE systems (1, 2) has facilitated analysis of the wave propagation and detection processes. However, the generation of elastic waves may be associated with a variety of events e.g. slip-band formation, particle rupture, mechanical twinning and crack growth, and the importance of a particular event as a source of AE will depend on the microstructure of the material. The relationship between the microstructure and the generation of AE during failure requires to be better characterized and understood if more reliance is to be placed on AE.

Aluminium alloys are extensively used in the aerospace industry and have been the subject of numerous AE studies (3–6). The material examined in this study is the high-strength alloy 7050. It was recently developed primarily for thick-section applications, has good stress-corrosion resistance, and is now being used in airframe construction. In this report, we present our AE results for this alloy and compare them with reported observations on similar materials. Emphasis is placed on the relationship between AE characteristics and the alloy microstructure, and its implications for source identification.

2. ALLOY MICROSTRUCTURE

The alloy 7050 is of the Al–Zn–Mg–Cu type, having approximate composition (wt.%) 6·2 Zn, 2·2 Mg, 2·3 Cu; it also contains 0·1 wt.% Zr (in place of Cr in the related 7075 alloy) as a recrystallization and grain control addition.

The alloy was received as a 76 mm thick, rolled slab in condition T7351, i.e. solution-treated at 480°C, quenched into water at room temperature, aged at 120°C for 4 hours, stretched 2%, and aged for 4 hours at 168 C. Visual inspection of a polished and etched section normal to the rolling direction revealed a variation in microstructure through the slab. The appearance of etched sections parallel to the rolling plane confirmed this variation (Fig. 1). Examination at higher magnifications showed that centre-layer material (C-material) had grains with two different sizes (corresponding approximately to ASTM Average Grain Size Nos 4 and 10) while outer-layer material (O-material) had an almost uniformly fine grain size (approx. No. 10); Figs 2 and 3 show examples.

Differences in texture were also observed: O-material had a single ⟨110⟩ texture parallel to the rolling direction, while C-material had a duplex texture, predominantly ⟨112⟩ with some ⟨100⟩.

A second feature of the microstructure is the presence of intermetallic particles; these particles have a wide range of sizes and a typical distribution of those above about 0·4 μm is shown in Fig. 4. All the intermetallic particles, together with the grain size and dislocation arrangement, help to determine the mechanical behaviour of the alloy. The particles can be classified according to the way they form (7, 8):

(a) Those which form during ingot solidification are usually termed constituent particles. They are partly broken up during subsequent fabrication but cannot be redissolved unless the alloy is entirely re-melted. They arise because of Fe and Si contents which, though small, are in excess of their solubility limits. Their size is usually in the range 0·1 to 20 μm.

(b) Those formed during homogenization of the alloy are usually called dispersoids. Once formed they cannot be redissolved, although their size and distribution can be modified

by high-temperature mechanical treatments. They inhibit recrystallization and grain growth during high-temperature fabrication. In most 7000-series alloys the dispersoids are chiefly Cr-based, but in 7050 they are Zr-based. Their sizes range from about 0·05 to 0·5 μm.

(c) Particles which form during ageing are usually called precipitates. They are metastable or equilibrium compounds of the major alloying elements, and range in size from about 0·002 to 0·05 μm. They determine the resistance to plastic flow of the alloy.

Most large particles (those above about 4 μm in the longest dimension) in our 7050 sample were elongated approximately parallel to the rolling direction, and often occurred in groups. The majority were light grey in colour; these were determined to be Fe-rich by energy-dispersive X-ray analysis. Dark-coloured large particles were also seen, and most of these were found to be Si-rich. These large constituent particles may also contain Al, as well as one or more of the major alloying elements (Cu, Mg, Zn). In sections parallel to the rolling plane the quantity, shape and orientation of the larger particles appeared very similar in C- and O-material (Figs. 5 and 6). However, in the section normal to the rolling direction, the dimensions of the particles were significantly less in O- than in C-material. Moreover, the number of smaller particles (those less than about 1 μm in size) was appreciably higher in O- than in C-material. Most, if not all, the particles above about 0·5 μm were of the constituent class. The magnifications used did not allow us to determine the classification of particles smaller than this, but some of those just visible (i.e. about 0·1 μm) in Figs. 5 and 6 may be dispersoids, the remainder of the visible ones being small constituent particles.

3. TESTING PROCEDURE

Specimens for tensile testing were cut with their faces parallel to the rolling plane of the slab and tensile axes parallel to the rolling direction. Specimen dimensions and location of the transducer are given in Fig. 7. In order to eliminate spurious emission during testing, the pins and loading-yoke were teflon-coated and the pin-holes were pre-stressed by inserting a rod and compressing the end of the specimen with a load well in excess of the subsequent maximum test-load. The transducer was coupled to the specimen with silicone-grease and, after its attachment, the specimens were strained at a constant extension rate of 0·02 mm s^{-1}.

A number of flawed specimens were also tested. These included single-edge-notched plates (dimensions shown in Fig. 7), and tensile specimens with a 1·5 mm diameter hole in the middle of the gauge-section.

Measurements of AE count-rates were made using a Dunegan/Endevco D9203 differential piezoelectric transducer with a resonant frequency of 175 kHz, a Dunegan/Endevco 802PA differential pre-amplifier with band-pass 100–300 kHz and a gain of 60 dB, and a GR counter with trigger level set at 18 mV and gate-time set to a period of 1 sec. A Biomation 8100 waveform recorder was included in this system for measurement of AE waveform. Spectral analysis was carried out using a broad-band Dunegan/Endevco S9201 transducer, a pre-amplifier with a uniform gain of 60 dB within the frequency range 0·2–1·0 MHz, the Biomation 8100 waveform recorder and an HP 8556A 8552B spectrum analyser.

4. AE COUNT-RATE MEASUREMENTS

Figure 8 shows typical load time and count-rate/time graphs for unflawed O- and C-specimens. In both cases detectable emission started at yielding; the count-rate rose swiftly to a maximum and then decayed. Although the load/time charts of the two types of material were very similar, much higher count-rates were detected from C-material specimens.

If a test was interrupted by unloading and reloading, counting was not observed until plastic flow recommenced. A test run at ten times the usual extension rate simply gave a tenfold increase in counts per unit time.

Some tensile specimens were solution-treated in a salt-bath at 480 C for 2 hours, quenched into water at room temperature, and then aged for 4 hours at 120 C. Tests of these specimens gave AE very similar to that shown in Fig. 8 from specimens in the T7351 condition. The count-

rates from C-material were again well in excess of count-rates from O-material. These results indicate that differences in the count-rate between C- and O-material were not associated with possible differences in aged microstructure due to different quench-rates experienced in the inner and outer regions of the original billet.

Further specimens were tested immediately after quenching. Load/time and count-rate/time records for these freshly quenched samples (Fig. 9) were quite different from those for T7351 specimens. The load/time curves were noticeably serrated, and there were sudden temporary increases in count-rate. Careful comparison of the records showed that each spike in the count-rate corresponded to a load-drop, but not all load-drops gave a sudden rise in detected rates of emission. There was no simple correlation between the size of the load-drop and the increase in count-rate. Substantially greater count-rates were observed from specimens in the as-quenched condition than from artificially-aged specimens.

To see if the differences in count-rate between O- and C-material extended to flawed specimens, a number of tensile specimens, each having a hole in the middle of the gauge-section, were tested at a cross-head speed of 0·01 mm s^{-1}. Deformation was localized at the hole in each case and fracture occurred there quite rapidly. Figure 10 shows count-rate/time charts for O- and C-specimens. The AE from the flawed C-specimen resembled the form of count-rate/time record obtained from the unflawed specimens. However, the flawed O-specimen showed a different behaviour with counts being obtained at random intervals. Emission from single-edge-notched plates is shown in Fig. 11. As in the case of unflawed specimens, more counts were observed in C- than O-specimens. As the load was increased, the count-rate increased in the C-specimen but remained almost constant in the O-specimen. No propagation of the flaw occurred, but plastic deformation around the tip was clearly visible in each case. These preliminary investigations of 7050 specimens with hole and notch flaws indicate that microstructure affects AE from plastically deforming material not only in a simple tensile specimen but also at the tip of a crack.

5. WAVE PROPAGATION

Our results show that the count-rate from 7050 alloy deforming plastically in simple tension is sensitively dependent on accumulated plastic strain. The reduction in count-rate with increasing plastic strain beyond the peak could arise either from a difference in generation of elastic waves or from an increase in the attenuation suffered by the waves as they propagate from the generation site to the transducer. A simple test was carried out to differentiate between these effects. Two identical C-specimens were prepared, each having a waisted section of 3·8 mm width and 20 mm length. One of these specimens was strained about 6% in tension; in agreement with the behaviour shown in Fig. 8, the count-rate had fallen to 7% of the peak value after this preliminary extension. A second waisted section of 2·0 mm width and 16 mm length was then machined in each specimen, and each was then strained in tension. Plastic flow was confined to the thinner test-section, as the load required to sustain plastic flow in the thin section was well below the yield load of the thicker test-section. The specimen with a pre-strained thick test-section gave a similar count-rate to the specimen with an unstrained thick test-section. This result would not be observed if count-rate reduction with increasing strain were caused by increased attenuation. Thus the effect of attenuation of elastic waves due to plastic strain is not significant in the frequency range of 100–300 kHz.

Further tests were carried out to determine whether the count-rate differences between specimens of C- and O-material should be attributed to differences in generation or propagation of elastic waves. The effects of wave propagation were studied by using a helium jet as a simulated AE source (2, 9). With the S9201 transducer located as shown in Fig. 7, the helium jet was applied to the centre of the gauge-section of each specimen and a spectral calibration obtained for the AE system. Specimens of C- and O-material gave similar spectra (see Fig. 12) and hence exhibited no difference in wave propagation characteristics. This result is also to be expected from basic considerations of the measurement frequency and the fairly isotropic elastic properties of the alloy (10).

6. THE SOURCE OF AE IN 7050

In the previous sections, we have illustrated that AE detected in both flawed and unflawed 7050 is dependent in some way on the microstructure of the alloy. We have also shown that this dependence arises from the generation, rather than the propagation, of AE. We therefore consider possible sources of AE in 7050.

6.1 Dislocation Motion

Our results appear to fit a general pattern, viz. the greater the difficulty of large-scale dislocation movement, the lower the count-rate. This conclusion applies whether the restriction to movement is brought about by plastic strain (see all unflawed-material results), by reduced grain-size (compare C- with O-material), or by forming precipitates (compare the freshly quenched with the aged 7050). Similar dependences of AE activity have been reported by many other workers (4, 11, 15). We note that the short-lived variations in count-rate from freshly quenched specimens are related to the discontinuous extensions which occur in this type of material; they do not necessarily indicate a change in the kind of source event (3, 16).

The existence of the above pattern suggests that the dislocation movement itself is the AE source in 7050. Indeed, the general trend in the pattern can be qualitatively explained if we assume that resistance to slip increases with decreased dislocation path-length, for this in turn alters the time duration and strain contribution of each slip event. Furthermore, the form of the count-rate time curves for both O- and C-specimens of 7050 closely resembles that from materials such as pure aluminium (11, 13), pure copper (17), and high-purity alloys (14, 15) in which the AE can be attributed unambiguously to dislocation movement. To check this comparison further, we examined voltage variations in signals captured by a transient recorder from a C-specimen of 7050-T7351 and a specimen of super-pure polycrystalline aluminium. (Unfortunately no comparative spectral analysis could be made, because the low signal amplitudes dictated the use of a resonant high-sensitivity transducer rather than a low-sensitivity broad-band transducer from which AE frequency characteristics could be derived). The signals were similar in that it was not possible to discern individual events in either case, so the AE can be regarded as continuous i.e. as having a sustained signal level produced by rapidly occurring events. This comparison lends further support to the suggestion that the AE source in 7050 is dislocation motion. However, the RMS voltages were considerably higher in the pure metal than in the alloy, resulting in much higher count-rates in the pure aluminium (a factor of about 7 higher than the count-rate in C-type 7050).

Certainly, elastic wave generation by large-scale dislocation motion could explain our results. However, we must also consider as an alternative AE source in 7050 the cracking of the hard intermetallic particles present in this alloy, since there is some evidence for this in previous AE studies of aluminium alloys (3, 5, 18, 19).

6.2 Particle Cracking

It is well established that constituent particles in commercial aluminium alloys provide sites for void formation via particle cracking or particle-matrix decohesion. The larger particles begin to crack at quite low strains (1-2%), and 25 to 50% are cracked after 7% strain (20). With continued straining, the voids grow and coalesce, causing fracture (20-24). In tensile specimens, only small amounts of void growth are observed, possibly due to the very small levels of triaxial tension in such specimens, compared with that at the crack-tip in a fracture toughness specimen. Consequently, void growth need not be considered as an AE source in our tests. The coalescence of the voids and the role of dispersoid particles in the process are more complex and are not well understood. As void coalescence is the final stage in the ductile fracture process, we need consider only constituent particle cracking when discussing AE generation, the bulk of which occurs at relatively low strains.

A range of aluminium alloys has been studied by Graham and Morris (3), who reported a qualitative correlation between AE level and the size and density of particles. They also reported comparatively lower count-rates from specimens machined from the outermost layers

of their thick plate samples, and suggested this was due to pre-test fracture of some of the particles in these outer layers. However, careful and extensive examination of our 7050 samples showed that particles in outer layers of this alloy were not cracked prior to testing (see Fig. 6), so the explanation of Graham and Morris cannot be applied to our results.

The most definitive method previously used to discriminate between possible AE sources involved comparison of AE generated during tensile and compressive deformation. The AE generated by dislocation motion is expected to be much the same in each case, whereas particle cracking should be far less frequent, or even absent, in compressive testing. Since AE RMS voltages were quite different during the two kinds of tests, which were performed on 2124-T851 (5) and 7075-T651, T6 (18, 19), the bulk of the AE was attributed to cracking of coarse particles (5, 18, 19). A very weak secondary AE peak was recorded for 7075-T6 (18, 19) and for the compression test of 2124 T851 (5), and this minor peak was thought to arise from dislocation movement. However, we note that in two of the studies mentioned above, different geometries were used for the compression and tension specimens (5, 18), with consequent differences in wave propagation and specimen resonance characteristics, while in the remaining test the transducer was mounted on the loading grips (19). Hence we feel these results cannot be interpreted unambiguously.

As previously noted, we found no evidence of any significant degree of cracking in the light grey Fe-rich particles in unstrained O- and C-material (see Figs. 5 and 6). However, it was very difficult to assess the amount of cracking in the dark Si-rich particles, in both strained and unstrained material. Most of these dark particles stood proud of the polished section, and boundaries common to adjacent facets could easily be mistaken for fine cracks.

A section from the gauge-length of a C-specimen which had been strained until peak count-rate had been reached was polished and examined. There was evidence of fine cracking perpendicular to the loading direction in some of the larger particles (Fig. 13). Sections from the gauge-lengths of fractured C- and O-specimens were also prepared and examined. Many of the particles in these samples were clearly cracked (Figs. 14 and 15) and often there were several cracks in the one particle. Decisions as to whether cracking was present could be made only for particles larger than about 1 μm. Some of our observations are thus compatible with AE generation based on particle cracking, especially as cracking is well under way by the stage that the peak in the count-rate is reached. Further quantitative metallography is needed before we can determine if the particles are present in sufficient number to account for the detected AE from 7050. (Our preliminary estimates indicate that the density of large void-producing particles in 7075, as determined by Van Stone *et al.* (20), is probably high enough to account for observed count-rates (3) from that alloy.)

Other observations do not appear compatible with the proposal that particle cracking is the AE source. Thus, preliminary estimates show there are very similar numbers of cracked particles in strained C- and O-specimens, even though the cross-sections, normal to the rolling direction, of the larger particles are greater in C- than in O-material. We noted above our uncertainty regarding cracking of particles smaller than about 1 μm; we point out, though, that if cracking of these smaller particles does take place, and contributes to the detected AE, we would observe higher count-rates from O- than from C-specimens, in contradiction to experimental results. Also, our metallographic examinations show that extensive particle cracking continues after the peak in the count-rate, so there is some doubt that particle cracking could account for the variation of count-rate with strain.

7. CONCLUSIONS

In this report we have examined the relationship between AE and microstructure in the aluminium alloy 7050. The trends apparent in our results can be qualitatively explained if we propose slip-band formation as the AE source in this alloy.

Although cracking of large brittle particles may contribute to AE in other aluminium alloys, it is difficult to account for all our observations by proposing that particle cracking generates all, or the bulk of, AE detected from 7050.

Further quantitative metallography and carefully designed experiments are required to distinguish between these possible AE sources.

ACKNOWLEDGEMENTS

We wish to acknowledge the advice and assistance given to us by R. A. Coyle, M. D. Engellenner, S. P. Lynch, and J. F. Nankivell.

REFERENCES

1. Hsu, N. N., Simmons, J. A., Hardy, S. C. Materials Evaluation 35, 100–106 (1977).
2. Scala, C. M., Scott, I. G. Materials Note 123, Aero. Research Labs. (1978).
3. Graham, L. J., Morris, W. L. Presented at the ASNT 35th National Fall Conf. (1975).
4. Clark, G. Dept. Metallurgy and Materials Science Rept., Cambridge University (1977).
5. Hamstad, M. A., Bianchetti, R., Mukherjee, A. K. Eng. Fracture Mechanics 9, 663–674 (1977).
6. Pless, W. M., Bailey, C. D., Hamilton, J. D. Materials Evaluation 35, 41–48 (1977).
7. Staley, J. T. ASTM STP605, 71–103 (1976).
8. Rosenfield, A. R., Price, C. W., Martin, C. J., Thompson, D. S., Zinkham, R. E. AFML-TR-74-129 (1974).
9. McBride, S. L., Hutchison, T. S. Canadian J. Phys. 54, 1824–1830 (1976).
10. Krautkramer, J., Krautkramer, H. "Ultrasonic Testing of Materials" Springer-Verlag, Berlin (1969).
11. Fleischmann, P., Lakestani, F., Baboux, J. C. Materials Science and Eng. 29, 205–212 (1977).
12. Rouby, D., Fleischmann, P. phys. stat. sol. (a) 48, 439–445 (1978).
13. Kiesewetter, N., Schiller, P. phys. stat. sol. (a) 38, 569–576 (1976).
14. Kuribayashi, K., Kishi, T. Materials Science and Eng. 33, 159–163 (1978).
15. Wadley, H. N. G., Scruby, C. B. Metal Science 12, 285–289 (1978).
16. Pascual, R. Scripta Met. 8, 1461–1466 (1974).
17. Mintzer, S., Pascual, R., Volpi, R. N. Scripta Met. 12, 531–534 (1978).
18. Hamstad, M. A., Mukherjee, A. K. UCRL-77502, Lawrence Livermore Lab., Calif. (1975).
19. Carpenter, S. H., Higgins, F. P. Met. Trans. 8A, 1629–1632 (1977).
20. Van Stone, R. H., Merchant, R. H., Low, J. R. ASTM STP556, 93–124 (1974).
21. Hahn, G. T., Rosenfield, A. R. Met. Trans. 6A, 653–667 (1975).
22. Garrett, G. G., Knott, J. F. Met. Trans. 9A, 1187–1201 (1978).
23. Van de Kasteele, J. C. W., Broek, D. Eng. Fracture Mechanics 9, 625–635 (1977).
24. Broek, D. Eng. Fracture Mechanics 5, 55–66 (1973).

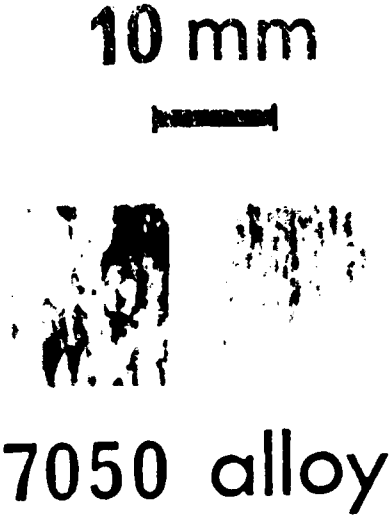

Fig. 1 Etched sections parallel to rolling plane; material from centre (C) layer of the billet is on the left, material from the outer (O) layers is on the right. Etched in solution of 5 ml HF, 20 ml HN03, 2 ml HCl, 100 ml water, combined, just before use, with equal volume of a 10% potassium dichromate solution.

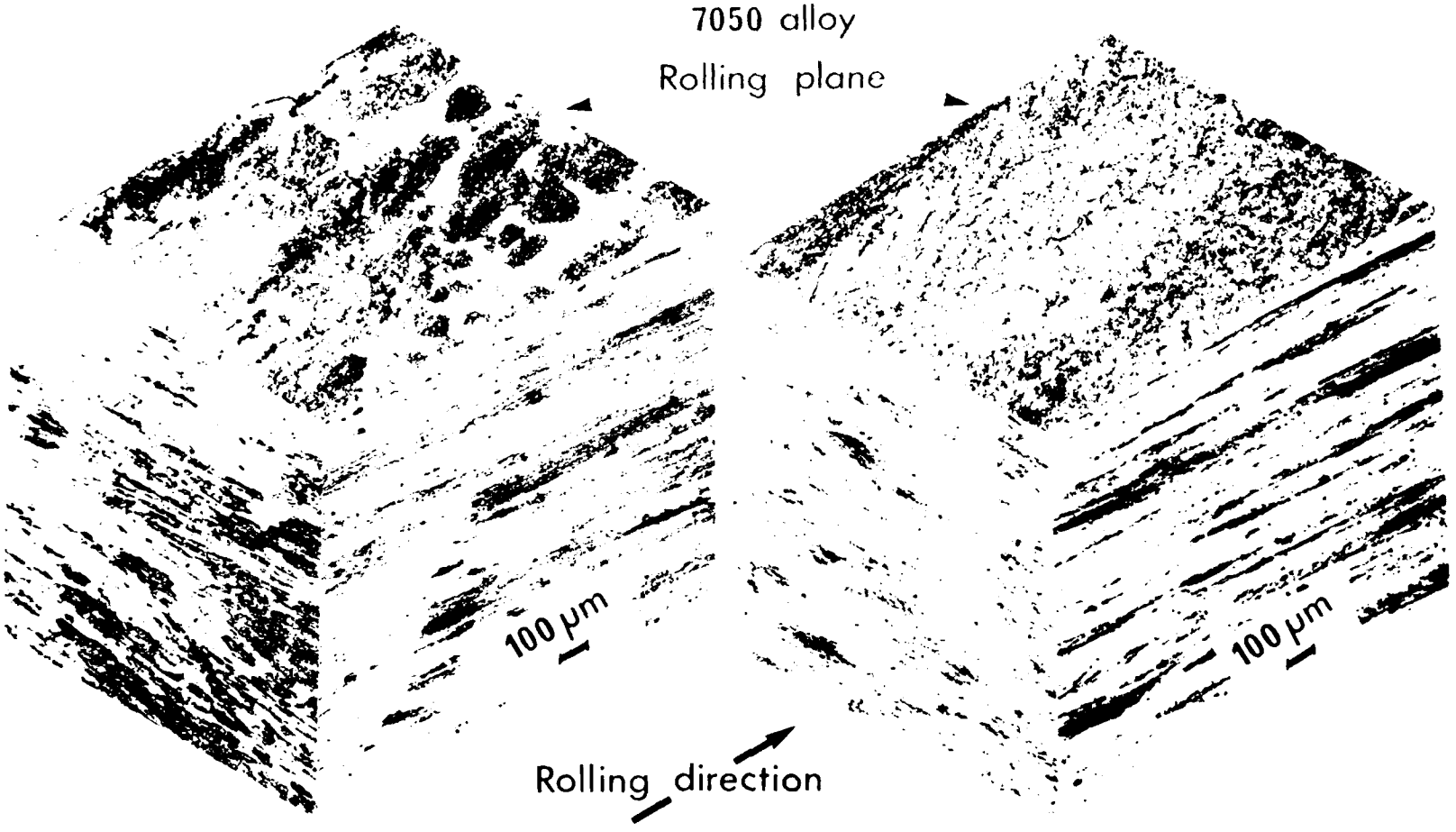

Fig. 2 Etched sections from C-material (left) and O-material (right) showing the general microstructure of the 7050 alloy. Etched as above.

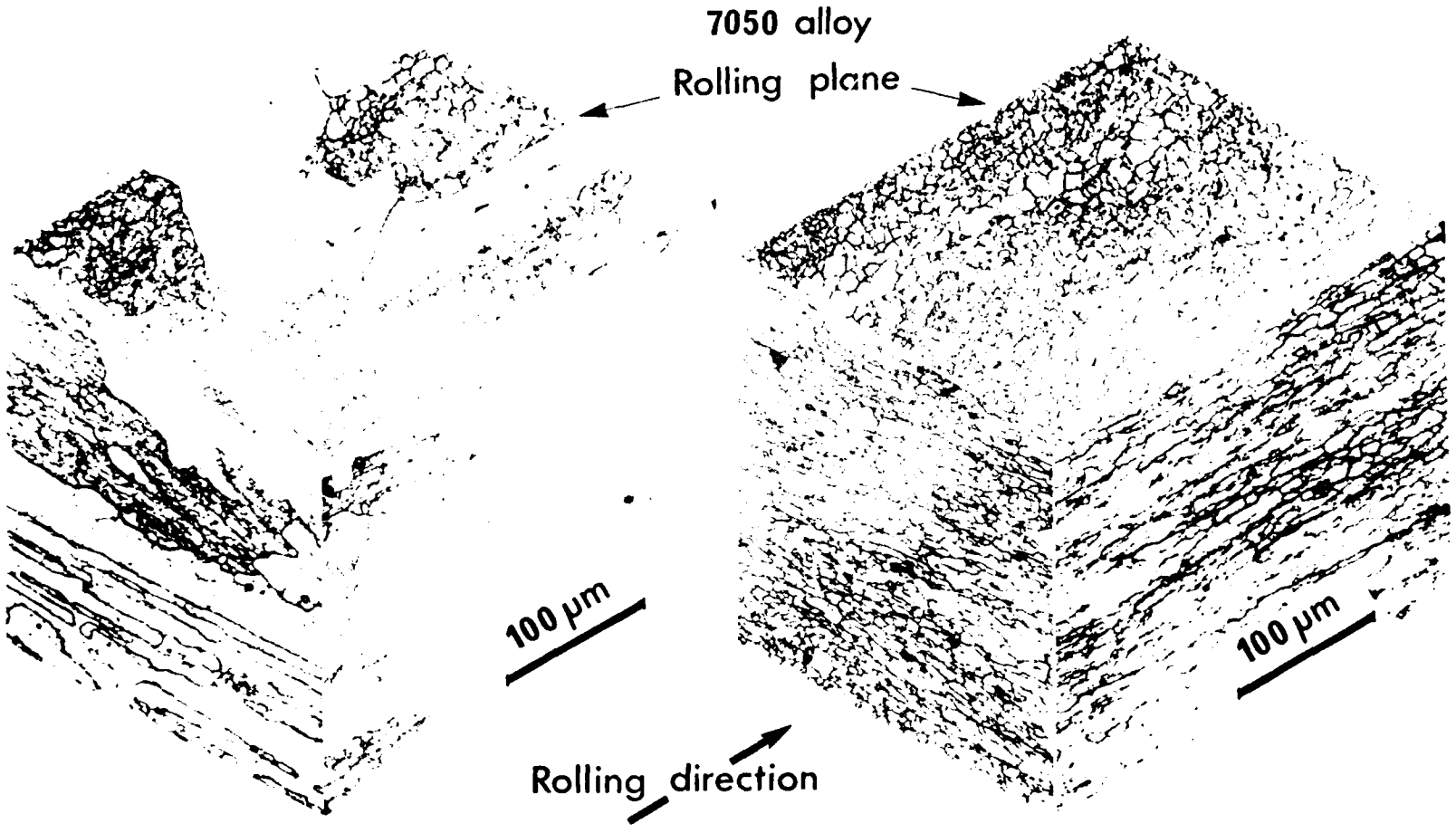

Fig. 3 As for Fig. 2, but at higher magnification to show grain sizes.

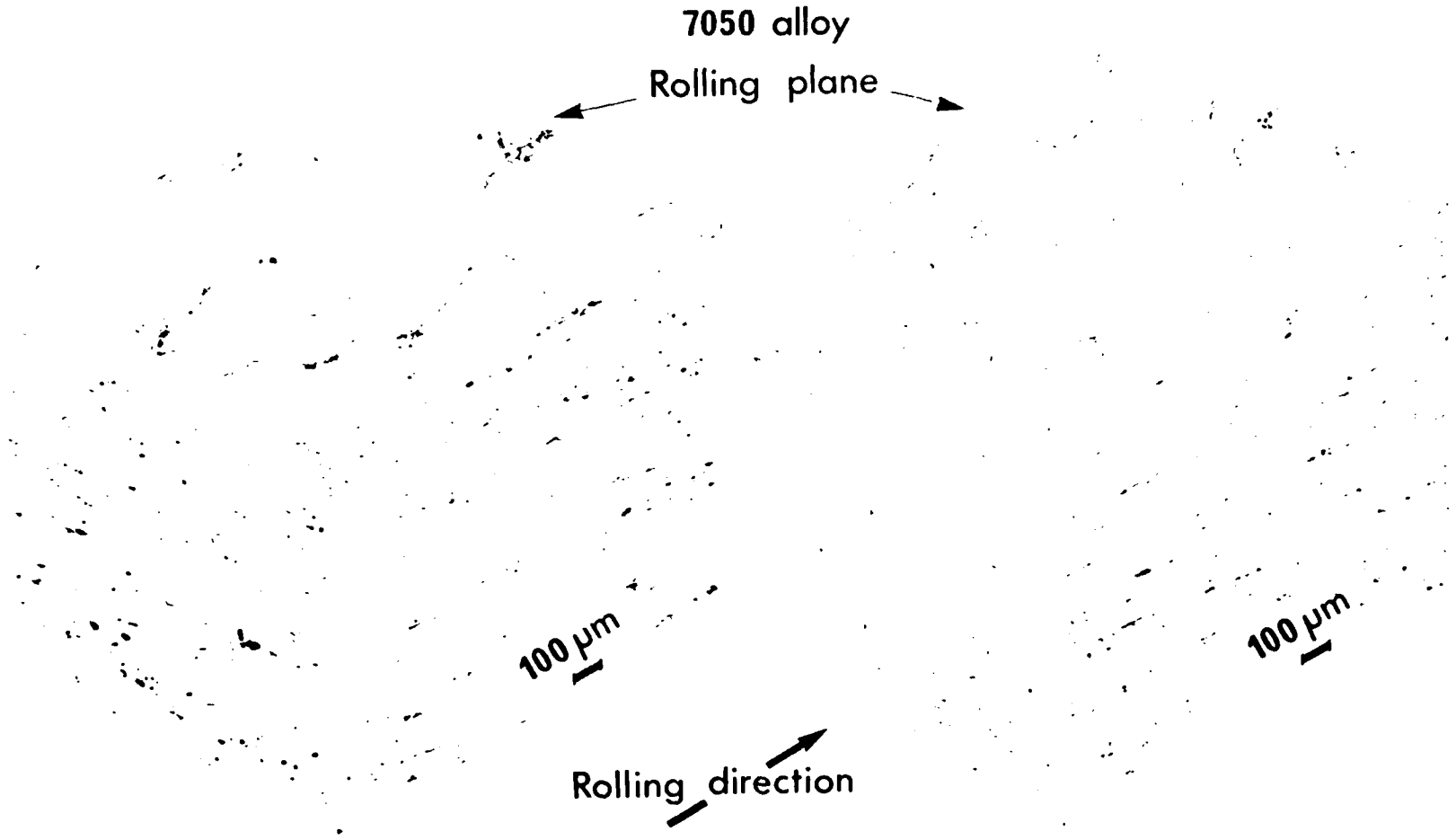

Fig. 4 Distribution of intermetallic particles in C-material (left) and in O-material (right).

Fig. 5 Mechanically polished section, parallel to rolling plane, of unstrained C-material, showing large intermetallic particles.

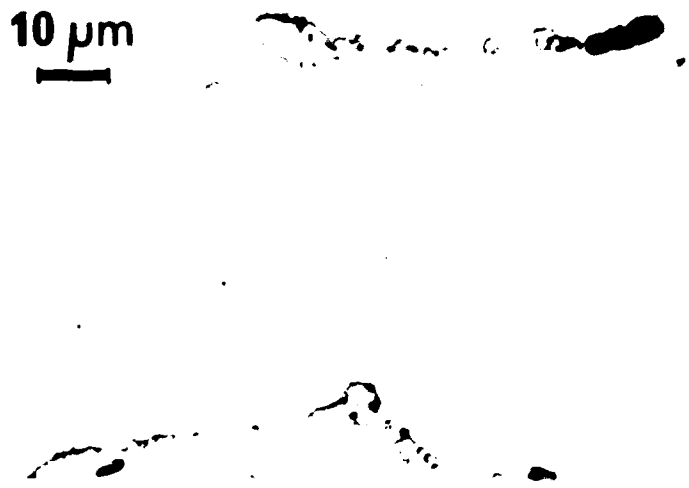

Fig. 6 Mechanically polished section, parallel to rolling plane, of unstrained O-material, showing large intermetallic particles.

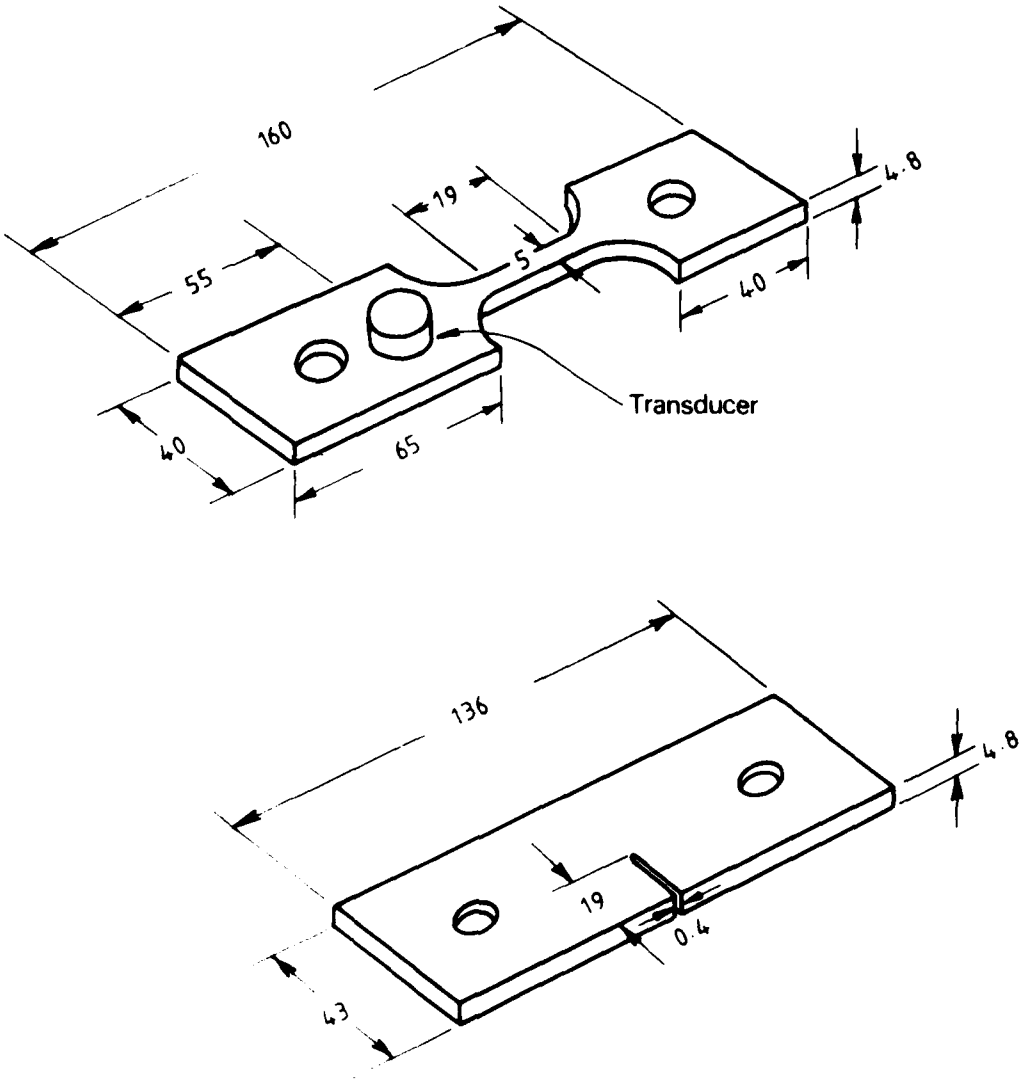

Fig. 7 Tensile specimen and SEN specimen; dimensions in mm.

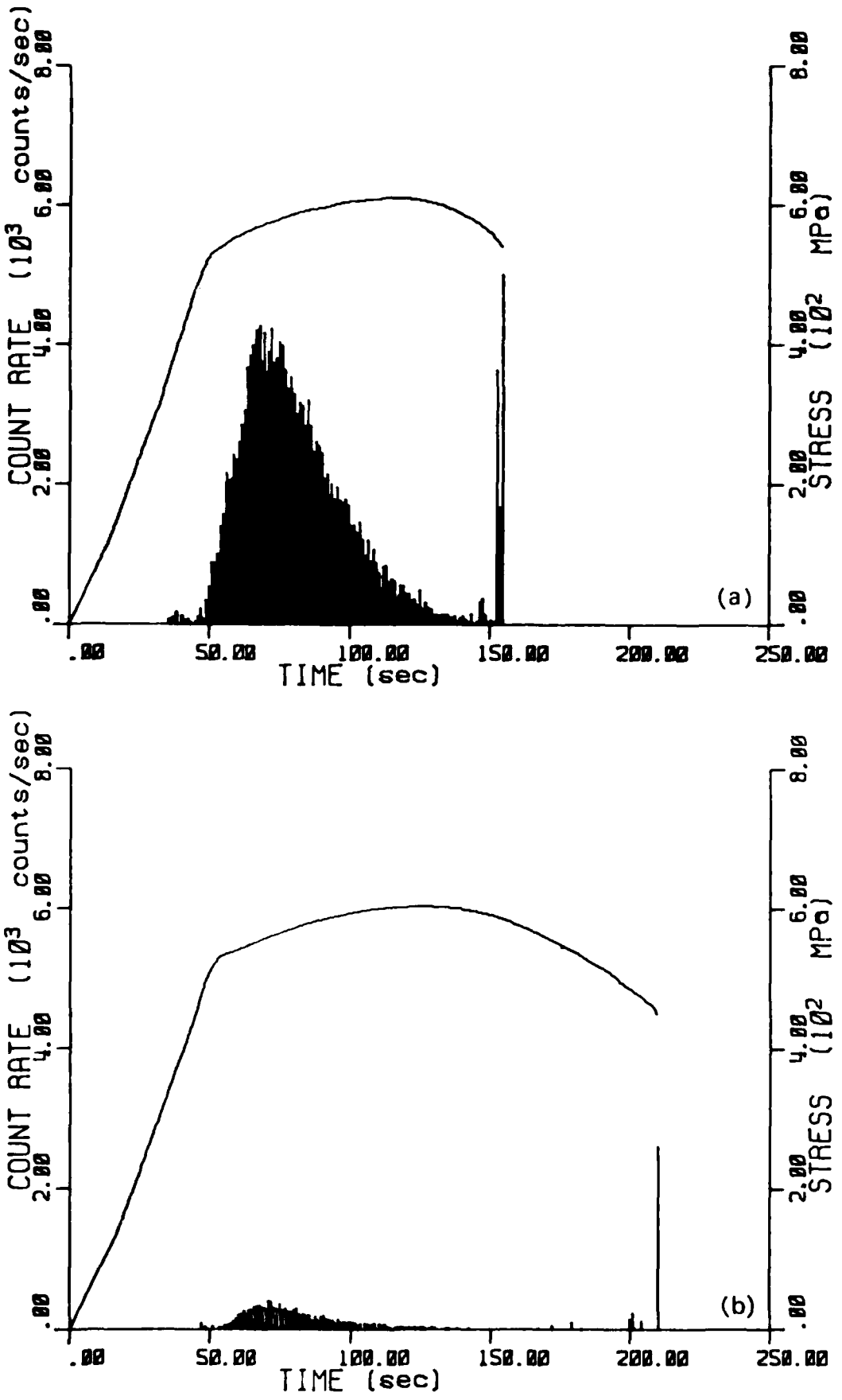

Fig. 8 Count-rate/time and nominal-stress/time curves for 7050 C-specimen (a) and O-specimen (b).

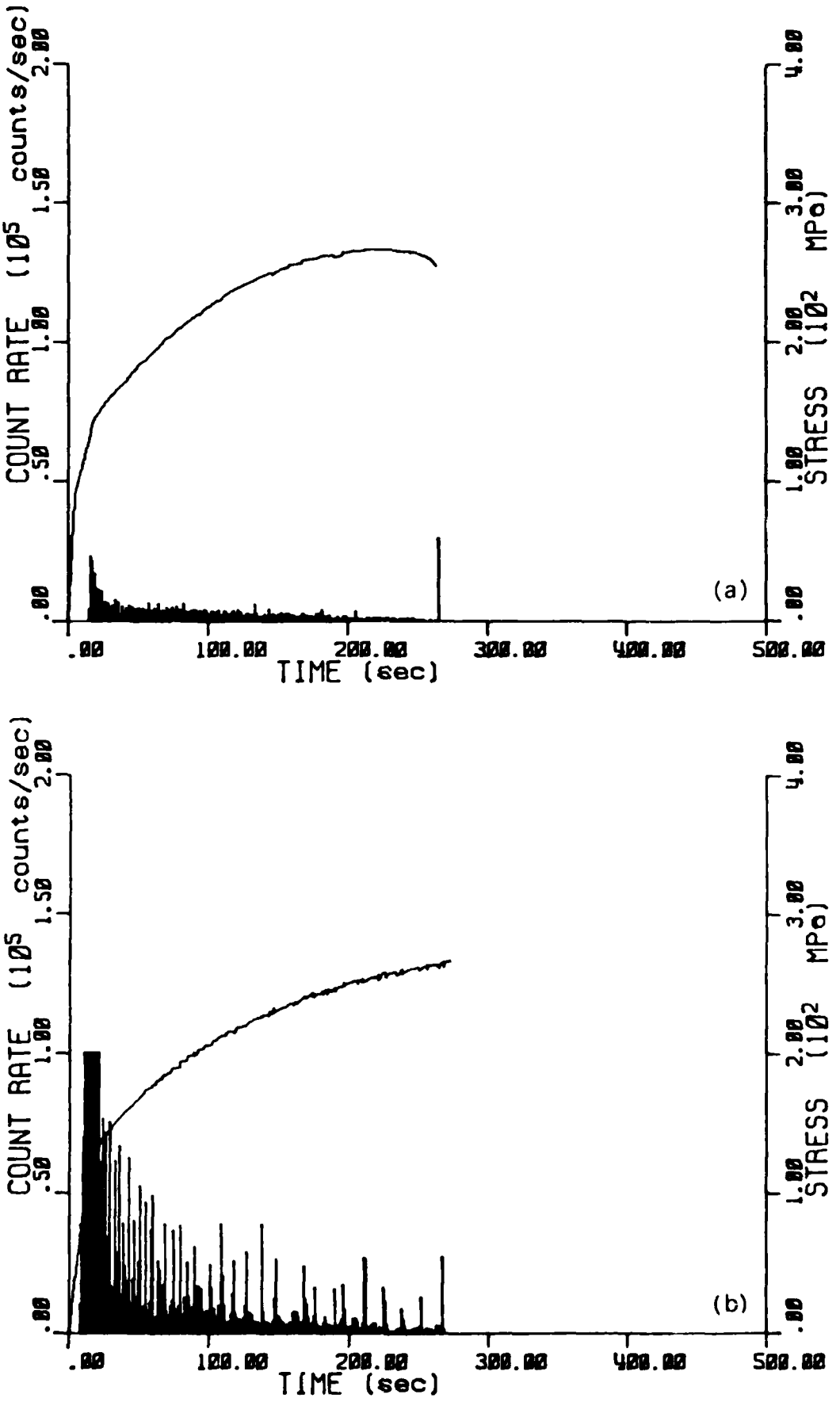

Fig. 9 Count-rate/time and nominal-stress/time curves for as-quenched 7050 C-specimen (a) and O-specimen (b).

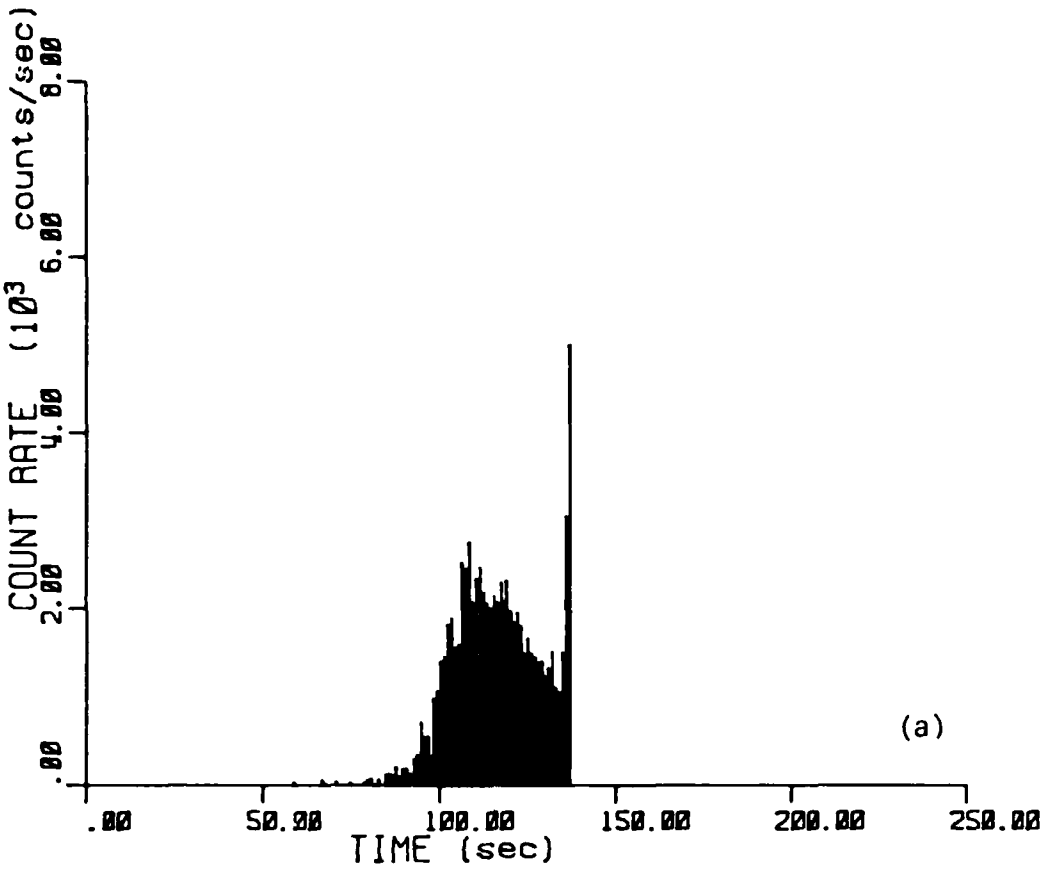

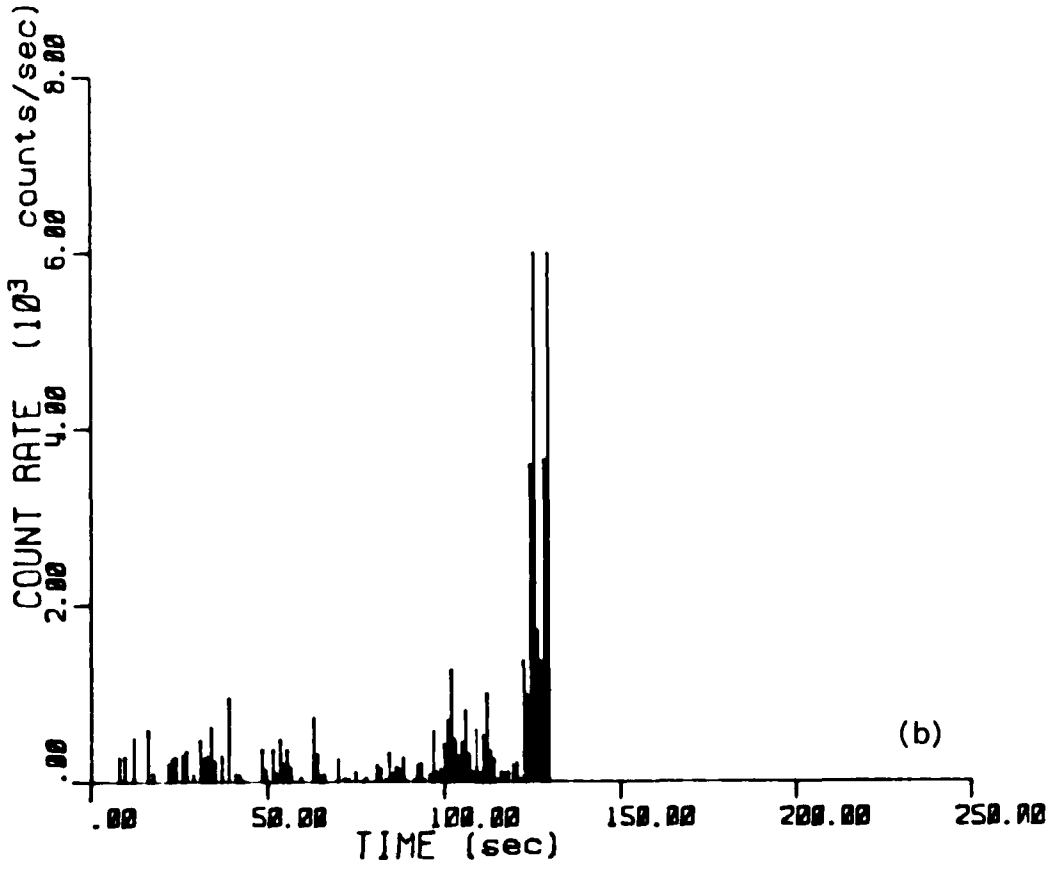

Fig. 10 Count-rate/time curves for 7050 C-specimen (a) and O-specimen (b), each having a

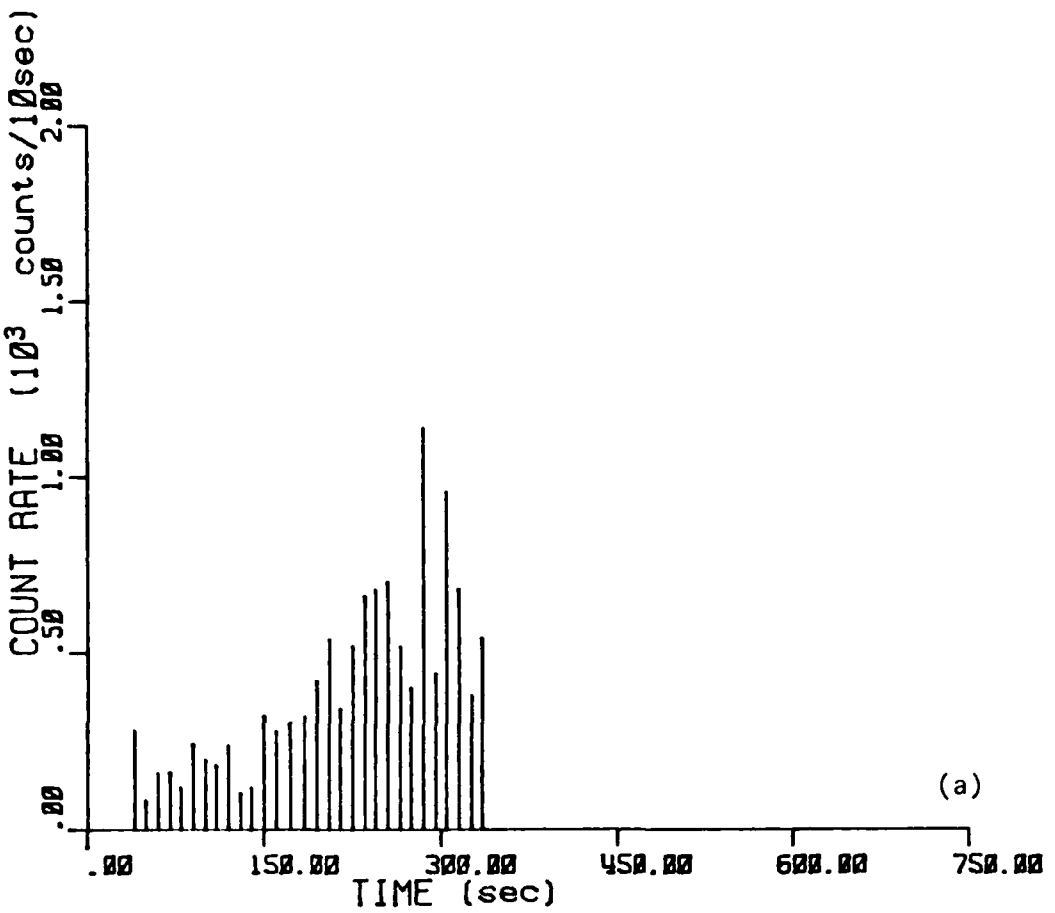

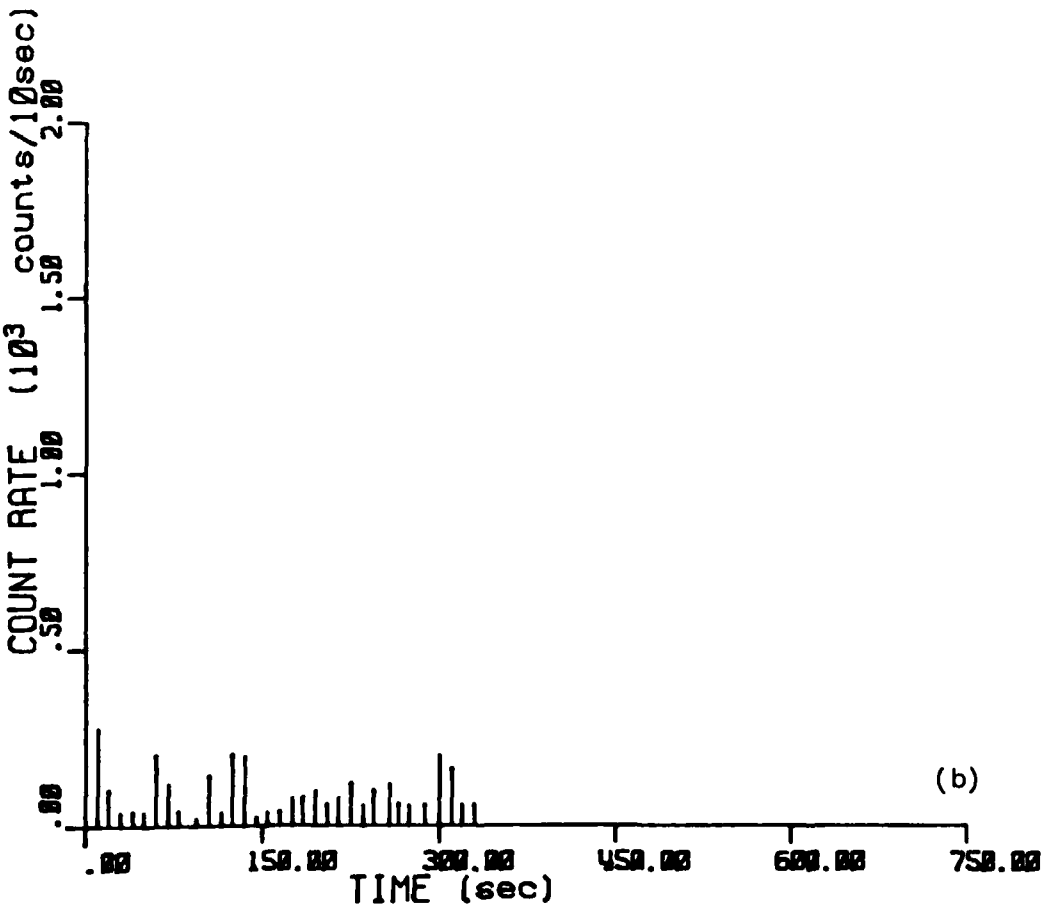

Fig. 11 Count-rate/time curves for 7050 SEN C-specimen (a) and O-specimen (b).

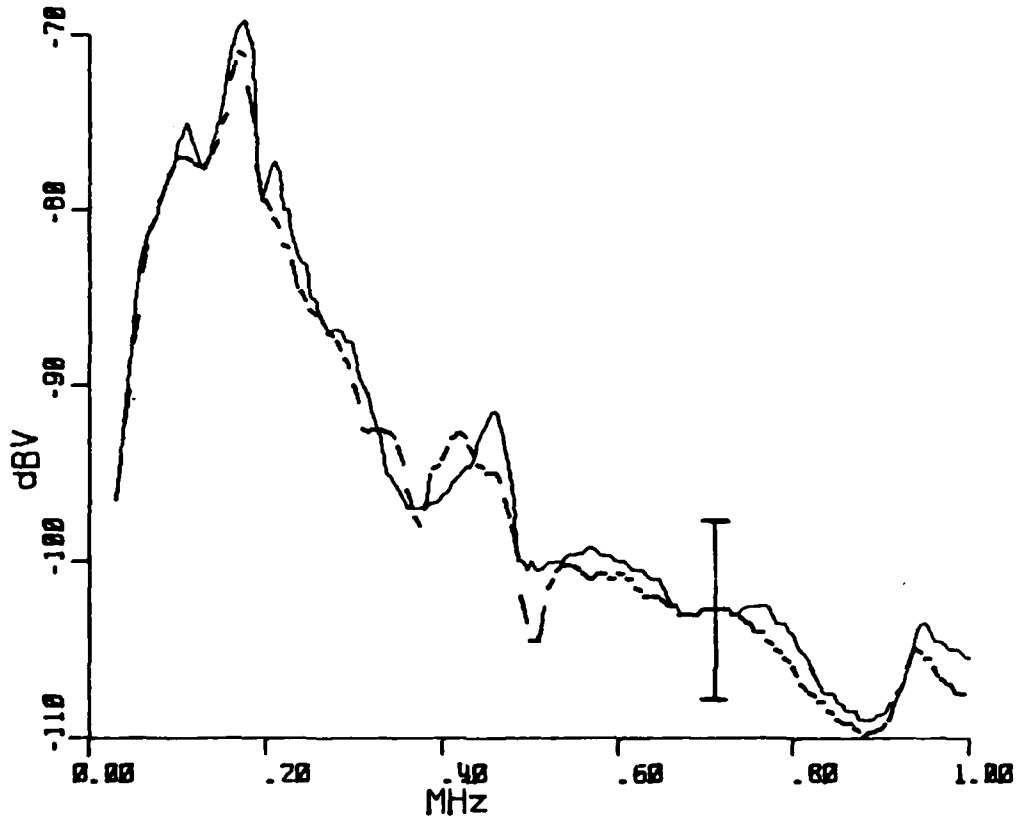

Fig. 12 Helium-jet spectral calibration of 7050 C-specimen (continuous line) and O specimen (dashed line).

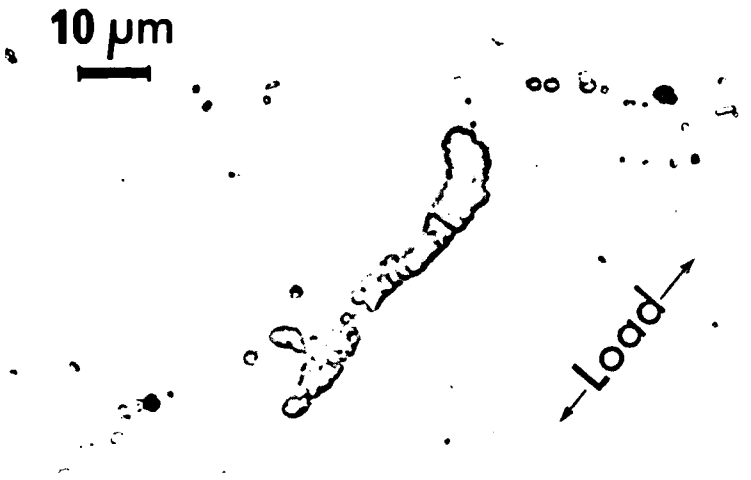

Fig. 13 Mechanically polished section, parallel to rolling plane, from C-specimen strained to peak count-rate.

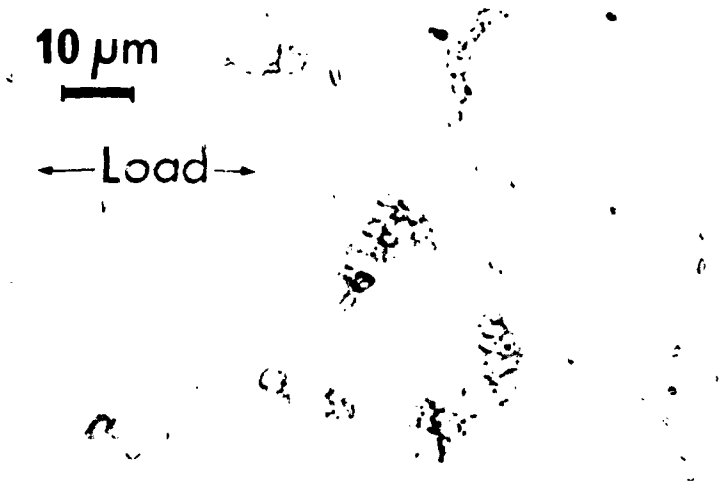

Fig. 14 Mechanically polished section, parallel to rolling plane, from C-specimen strained to fracture.

Fig. 15 Mechanically polished section, parallel to rolling plane, from O-specimen strained to fracture.

DISTRIBUTION

	Copy No.
AUSTRALIA	
Department of Defence	
Central Office	
Chief Defence Scientist	1
Deputy Chief Defence Scientist	2
Superintendent Science and Technology Programs	3
Australian Defence Scientific and Technical Representative (UK)	—
Counsellor, Defence Science (USA)	—
Joint Intelligence Organisation	4
Defence Library	5
Assistant Secretary, D.I.S.B.	6–21
Aeronautical Research Laboratories	
Chief Superintendent	22
Library	23
Superintendent — Materials Division	24
Divisional file Materials	25
Authors: S. McK. Cousland	26
C. M. Scala	27
G. G. Martin	28
I. G. Scott	29
Materials Research Laboratories	
Library	30
Defence Research Centre, Salisbury	
Library	31
Central Studies Establishment	
Information Centre	32
Engineering Development Establishment	
Library	33
RAN Research Laboratory	
Library	34
Defence Regional Office	
Library	35
Navy Office	
Naval Scientific Adviser	36
Army Office	
Army Scientific Adviser	37
Royal Military College Library	38

INTERNATIONAL COMMITTEE ON AERONAUTICAL FATIGUE

Per Australian ICAF Representative 75-99

JAPAN

National Aerospace Laboratory, Library 100

NETHERLANDS

National Aerospace Laboratory (NLR), Library 101

NEW ZEALAND

Defence Scientific Establishment, Librarian 102
Transport Ministry, Civil Aviation Division, Library 103

Universities

Canterbury Library 104

SWEDEN

Aeronautical Research Institute 105

SWITZERLAND

Armament Technology and Procurement Group 106

UNITED KINGDOM

Mr A. R. G. Brown, ADR MAT (MEA) 107
Aeronautical Research Council, Secretary 108
CAARC, Secretary 109
Royal Aircraft Establishment:
- Farnborough, Library 110
- Bedford, Library 111
- Dr David Stone 112

Royal Armament Research and Development Establishment 113
Admiralty Marine Technology Establishment, Mr D. Birchon 114
British Library, Science Reference Library 115
British Library, Lending Division 116
CAARC Co-ordinator, Structures 117
Central Electricity Generating Board 118
Welding Institute, Library 119

UNITED STATES OF AMERICA

NASA Scientific and Technical Information Facility 120
Nondestructive Testing Information Analysis Centre 121
Metals Abstracts, Editor 122
Battelle Memorial Institute, Library 123
Battelle Northwest Laboratories, Mr P. H. Hutton 124
Naval Sea Systems Command, Dr H. H. Vanderveldt 125
Naval Air Development Center, Dr J. M. Carlyle 126
Naval Research Laboratory, Mr S. Hart 127
Rockwell International Science Center, Dr L. J. Graham 128
Defence Advanced Research Projects Agency, Dr M. J. Buckley 129
National Bureau of Standards, Dr N. N. Hsu 130

Spares 131-140


DATE
ILME